

Article

Characteristics and Environmental Indications of Grain Size and Magnetic Susceptibility of the Late Quaternary Sediments from the Xiyang Tidal Channel, Western South Yellow Sea

Fei Xia ^{1,*} , Dezheng Liu ² and Yongzhan Zhang ³

¹ School of Geography, Jiangsu Second Normal University, Nanjing 211200, China

² School of Ocean Engineering and Technology, Sun Yat-Sen University, Zhuhai 528478, China; dezhen_lu@126.com

³ The Key Laboratory of Coast and Island Development of Ministry of Education, School of Geography and Ocean Science, Nanjing University, Nanjing 210023, China; zhangyzh@nju.edu.cn

* Correspondence: feixia@jssnu.edu.cn

Abstract: To reveal the characteristics and environmental indications for the combination of the grain size and magnetic susceptibility of coastal sediments, we provided a necessary basis for further study on their genetic mechanisms. Based on the data of grain size and magnetic susceptibility of the 36.10 m long core 07SR01 sediments in the Xiyang tidal channel of western South Yellow Sea, we analyzed their variations and correlations and further revealed their environmental indications and corresponding regional sedimentary evolution via the combination of the aforementioned analysis results, the reinterpretation results of the sedimentary sequence and the age of core 07SR01 and shallow seismic profiles, and the findings of climate and glacial–eustatic cycles during Late Quaternary. The three stages of the sedimentary evolution of the Xiyang tidal channel between marine isotope stage (MIS) 7 and MIS 5 were summarized as follows: First is the stage of marginal bank and riverbed developments in the tidal estuary under a relatively high sea level and strong hydrodynamic conditions during MIS 7 (core section: 36.10–26.65 m). The sediments deposited in this stage were mainly affected by the paleo-Changjiang River and characterized by a coarse grain size (mean: 4.02 Φ) and relatively high magnetic susceptibilities (mean: $27.06 \times 10^{-8} \text{ m}^3 \cdot \text{kg}^{-1}$), with small fluctuations which were strongly and positively correlated with the sand component. Second is the stage dominated by fluviolacustrine and littoral environments with the weak hydrodynamics during MIS 6–5, in which the climate changed from cold and dry to warm and humid as the sea level rose after a drop (core section: 26.65–15.77 m). The sediments deposited in this stage were characterized by a fine grain size (mean: 5.27 Φ) and low magnetic susceptibilities with minor variations (mean: $10.83 \times 10^{-8} \text{ m}^3 \cdot \text{kg}^{-1}$) which were weakly and positively correlated with the coarse silt component. Third is the stage of delta front in the tidal estuary with a relatively high sea level and strong hydrodynamics during MIS 5 (core section: 15.77–0 m). The sediments deposited in this stage were strongly influenced by the paleo-Yellow River and characterized by a relatively coarse grain size (mean: 4.86 Φ), and high magnetic susceptibilities (mean: $37.15 \times 10^{-8} \text{ m}^3 \cdot \text{kg}^{-1}$) with large fluctuations which were weakly and positively correlated with the sand and coarse silt components.

Keywords: grain size; magnetic susceptibility; environmental indication; Late Quaternary; South Yellow Sea; Jiangsu coast



Citation: Xia, F.; Liu, D.; Zhang, Y. Characteristics and Environmental Indications of Grain Size and Magnetic Susceptibility of the Late Quaternary Sediments from the Xiyang Tidal Channel, Western South Yellow Sea. *J. Mar. Sci. Eng.* **2024**, *12*, 699. <https://doi.org/10.3390/jmse12050699>

Academic Editor: Anabela Oliveira

Received: 7 March 2024

Revised: 16 April 2024

Accepted: 18 April 2024

Published: 24 April 2024



Copyright: © 2024 by the authors. Licensee MDPI, Basel, Switzerland. This article is an open access article distributed under the terms and conditions of the Creative Commons Attribution (CC BY) license (<https://creativecommons.org/licenses/by/4.0/>).

1. Introduction

As the most basic and main physical characteristics of sediments, grain size is mainly affected by factors such as the transport medium, sediment dynamics, and provenance and is very sensitive to changes in sedimentary environments. Therefore, the grain size characteristics of sediments can be used as an important physical indicator and an effective

proxy for discriminating the sedimentary environments [1–4]. The environments in which the sediments were formed can be well revealed on the basis of their grain size composition, parameters and illustrations [5,6]. In estuarine coastal areas, grain size has been widely used as an important parameter indicative of dynamic sedimentary environments. For example, Zhou et al. and Li et al. [7,8] analyzed and compared the sediment grain sizes of multiple column samples from the mouths of the Changjiang River and Yalujiang River, respectively, showing that variations in sediment grain size parameters are directly related to sediment dynamics, and larger changes in grain size parameters (sorting coefficient, skewness, and kurtosis) reflect more turbulent sedimentary environments, whereas smaller changes reflect more stable sedimentary environments. Deng et al. [4] studied the relationship between the grain size characteristics of core sediments and hydrodynamics in the Changjiang River estuary since the Last Glacial Period, showing that sedimentary environments with strong hydrodynamic conditions and large disturbances tend to have coarser sediment grain sizes, greater variability in sorting, unstable concentration degree of particulate components, and sharp peak shapes. Similarly, Pan et al. [9] conducted an elaborate analysis and comparison using the grain size data of core sediments since Late Quaternary in the Qiantangjiang River, showing that the grain size parameters under stronger hydrodynamic conditions are more variable with coarser grain sizes, poorer sorting, and narrower peaks in the frequency distribution curves.

The magnetic susceptibility of sediments can reflect the magnetic characteristics of materials in nature and can be used to analyze the spatial–temporal variations in magnetic minerals and their indications to provide information regarding environmental changes. Moreover, the measurement of magnetic susceptibility has the advantages of being fast and easy, economical, highly repeatable, non-destructive, and portable for the instrument [10,11]. Therefore, magnetic susceptibility rapidly became an important proxy for environmental changes, and it has received wide attention and been applied in the environmental studies of loess, lakes, and deep seas [11], while it has been applied later in the studies of estuaries, coasts, and deltas, where the sea–land interactions and sedimentary environments are complex and varied, but good research results have also been achieved. For example, Jia et al. and Zhang et al. [12,13] found that the magnetic susceptibility of estuarine core sediments can indicate the strength of hydrodynamics to a certain extent, indirectly reflecting the evolution of sedimentary environments, and a high value of magnetic susceptibility indicates stronger hydrodynamics, while a low value indicates weaker hydrodynamics. Ge [14] studied the magnetic susceptibility of core QC₂ sediments in the South Yellow Sea, showing that the variation characteristics of magnetic susceptibility basically reflect the variation pattern of climatic environments, i.e., the magnetic susceptibility increased relatively in the warm and humid period and decreased relatively in the cold and dry period. Based on the magnetic susceptibility study of four cores from the inner continental shelf of the Hong Kong Special Administrative Region, Yim et al. [15] argued that the magnetic susceptibility can provide the means of distinguishing between seabed sediments affected by shipping contamination and identifying the palaeosols formed by the subaerial exposure of marine isotope stage (MIS) 5 marine deposits during MIS 4–2. Meanwhile, the increase in magnetic susceptibility was explained by the development of acid–sulphate soils through the oxidation of pyrite into iron oxides and hydroxides [15]. Through a correlation analysis of the magnetic susceptibility of core LZ908 sediments and Quaternary sea level changes in the south coast of the Bohai Sea, Yao [16] found that the high magnetic susceptibilities correspond to the period of high sea levels, while the low magnetic susceptibilities correspond to the period of low sea levels.

Meanwhile, a very close correlation between sediment grain size and magnetic susceptibility has also been found and explored a lot in depth in previous studies [17–21]. Magnetic susceptibility is influenced by a variety of factors (sediment dynamics, early diagenesis, organic matter content, etc.), and these factors are also directly or indirectly influenced by climatic and environmental conditions [22–25]. Therefore, the correlation between grain size and magnetic susceptibility varies in different spatial and temporal

environments, and further exploration of the two proxies' correlation will, to a certain extent, help to identify the physical significance and variation process of magnetic susceptibility, as well as the paleo-environmental information embedded in the grain size and magnetic susceptibility, which is of great significance for revealing regional environmental changes. Since Late Quaternary, the middle Jiangsu coast has been under the long-term and continuous subsidence. Meanwhile, both the Changjiang River and the Yellow River have affected this area in different spatial and temporal combinations, so this area is very sensitive to sea level changes and sea-land environmental evolutions, and it is an ideal area for the study of deposits originated by the Late Quaternary river-sea interaction (Figure 1). Based on the data of the grain size and magnetic susceptibility of the 36.10 m long core 07SR01 sediments of the Xiyang tidal channel in the middle Jiangsu coast, western South Yellow Sea, we analyzed their variations and correlations and then further revealed their environmental indications and corresponding regional sedimentary evolution via the combination of the aforementioned analysis results, the reinterpretation results of the sedimentary sequence and age of core 07SR01 and shallow seismic profiles, and the findings of the climate and glacial-eustatic cycles of the Northern Hemisphere during Late Quaternary. This study could deepen the understanding of sedimentary evolution of the middle Jiangsu coast since Late Quaternary and also provide a necessary basis for further study on the genetic mechanisms of environmental indications for the combination of the grain size and magnetic susceptibility of coastal sediments.

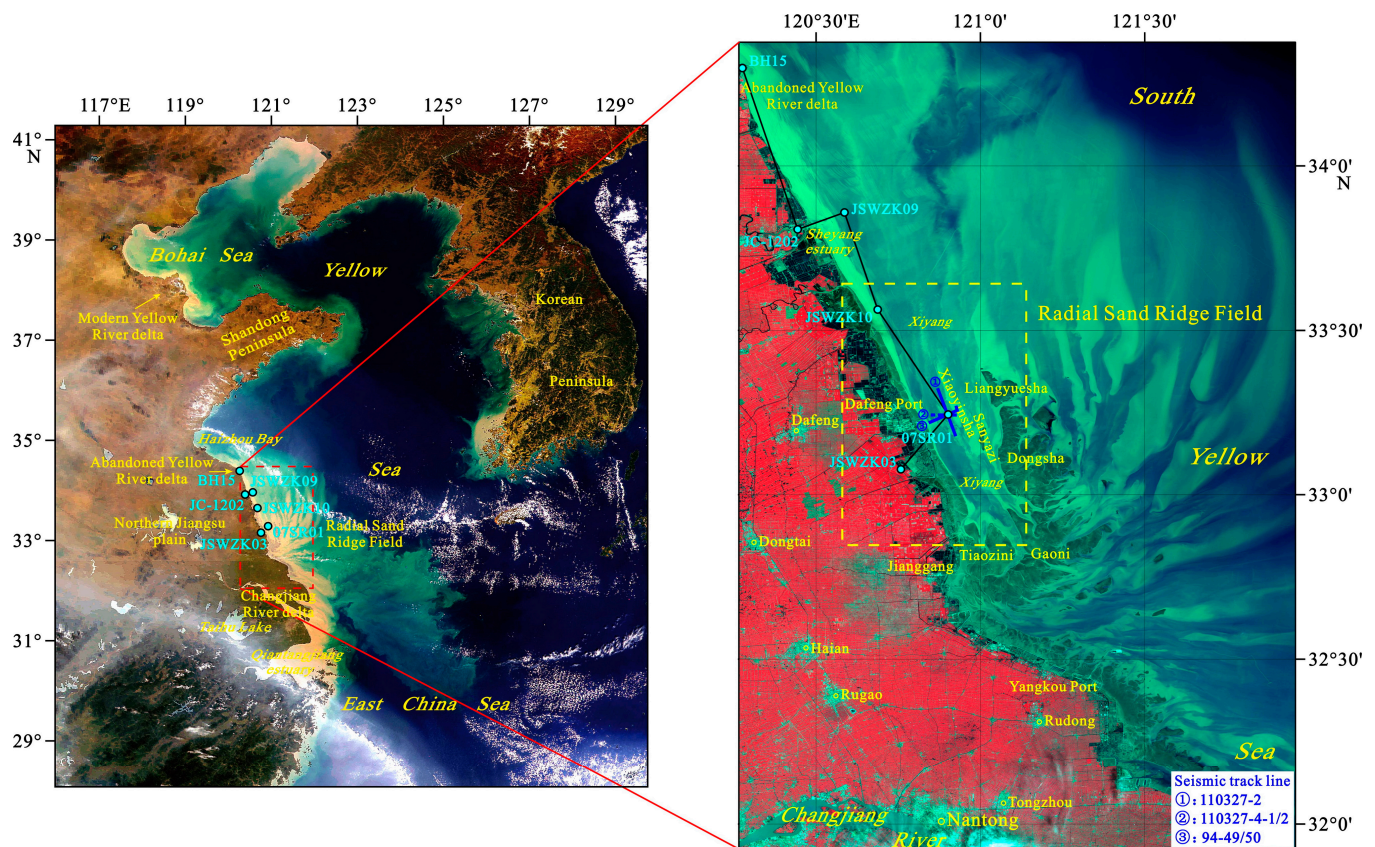


Figure 1. Remote sensing imageries of the Xiyang tidal channel in the middle Jiangsu coast, western South Yellow Sea and its adjacent regions, and locations of sedimentary cores and track lines of shallow seismic profiles mainly studied in this paper; the blue line segments show the track lines of shallow seismic profiles; the cyan round dots show the locations of sedimentary cores.

2. Regional Settings

Regarding the regional geology, the northern part of the study area belongs to the Yaosha Sag in the Yanfu Depression, and the southern part belongs to the Xiaohai Uplift.

Meanwhile, both the Yanfu Depression and the Xiaohai Uplift belong to the basin of the northern Jiangsu–southern South Yellow Sea on the northern Yangtze Paraplatform [26]. Regarding the Yangtze Paraplatform on the Jiangsu coast, a large-scale Late Cretaceous–Cenozoic continental sedimentary basin based on the Paleozoic carbonate rocks since the Indosinian–Yanshan Movement has been discovered, and the loose Quaternary strata with the interbedded sediments of marine and continental facies are up to ca. 250 m thick in the study area [26]. Regarding the regional landforms, the study area is located on the Radial Sand Ridge Field (RSRF), which is off the Jiangsu coast, between the abandoned Yellow River delta and the Changjiang River estuary, and on the inner shelf of the western South Yellow Sea, with a length of ca. 200 km from north to south and a width of ca. 140 km from east to west. The RSRF is a large-scale combination of seafloor landforms on the modern coastal zone and inner shelf and consists of more than 70 sand ridges and corresponding tidal channels, which are generally spread to the sea in a folded fan-like manner with the Jianggang as the apex, and the ridges and grooves are distributed one after another, mostly with a water depth of 0–25 m, seldom exceeding 40 m [26,27]. The Xiyang tidal channel is located on the northwestern part of the RSRF, with the tidal flats of the middle Jiangsu coast on the west side, the Dongsha sand ridge which is the largest sand island of the RSRF on the east side, and the Liangyuesha sand ridge adjacent to the north side of the Dongsha sand ridge, and it extends in the direction of NNW-SSE, with a width of ca. 12–25 km and a length of ca. 80 km. The Xiyang tidal channel is divided into the east and west sub-channels by the Xiaoyinsha and Piaoersha sand ridges (Figure 1). The wave climate in the Xiyang tidal channel is dominated by wind waves and is not strong, with the dominated wave direction being N and the strongest wave direction being NE throughout the year. Affected by the regular semidiurnal tide, the average tide range in the Xiyang tidal channel is ca. 3.5 m. Under the control of the rotating tidal wave system in the South Yellow Sea, the strong reciprocating tidal current is dominant, and the speeds of the rising and falling tidal currents are both relatively large. However, the flow rate of the falling tide is larger than that of the rising tide, and the turnover time of the rising and falling tidal currents is very short, so it is unfavorable for the diffusion and sedimentation of sediments and beneficial for the maintenance of the deep channel with the maximal water depth exceeding 40 m [26–29]. In recent years, the Xiyang tidal channel has continued to widen and deepen by scouring, which is very conducive to the stable development of coastal port channels [30].

3. Materials and Methods

3.1. Sample Collection

The core 07SR01 (location: 33°15'50" N, 120°53'46" E; in situ-measured water depth: 22 m) studied in this paper was drilled within the west sub-channel of the Xiyang tidal channel of the RSRF by Nanjing University in December 2007. The diameter and drilling depth of core 07SR01 is 71 mm and 36.1 m, respectively, with a total core recovery of ca. 70% (Figure 1). The core was split along the longitudinal direction, with one half used for archival retention and the other half as a working core. The sampling for the grain size measurement was basically carried out at 10 cm intervals, and a total of 229 samples were obtained. The sampling for the magnetic susceptibility measurement was basically carried out at 20 cm intervals, and a total of 104 samples were obtained. Of these, 90 samples of grain size and magnetic susceptibility were sampled at the same depth.

3.2. Laboratory Analysis

The grain size measurement was completed in the Key Laboratory of Coast and Island Development of the Ministry of Education, Nanjing University, and the samples were measured using a Malvern Mastersizer 2000 laser particle size analyzer (Malvern Instruments Ltd., Worcestershire, UK). The range of the measured grain sizes was from 0.02 to 2000 μm , and the error of repeated measurements was generally <2%. All samples were pre-treated and tested in accordance with the methods and procedures required by

the Technical Regulations for Marine Bottom Sediment Investigation developed by the 908 Special Project of the State Oceanic Administration of China [31]. Meanwhile, each sample in the pre-treatment stage was the mixed and homogeneous one with a weight of 2 g. After obtaining the grain size distribution data of samples, four grain size parameters (i.e., mean grain size, sorting coefficient, skewness, and kurtosis) were calculated using the GRADISTAT software according to the formulas for graphic measures introduced by Folk and Ward [32].

The magnetic susceptibility measurement was carried out in the Laboratory of Earth Surface Process and Environment of Nanjing University. After the samples were dried at a low temperature (37 °C), dispersed (without damaging natural particles), and mixed homogeneously, they were weighed at ca. 10 g and loaded into a special test box of 10 cm³, and then the bulk magnetic susceptibility (10^{-5} (SI)) at a lower frequency (470 Hz) of the samples was measured using a Bartington MS2 magnetic susceptibility system with the MS2B dual-frequency sensor (Bartington Instruments Ltd., Witney, UK). In order to ensure the measurement accuracy, each sample was measured 5 times, including 3 times for the test box containing sediments (values κ_1 – κ_3) and 2 times for the air background (values b_1 , b_2), and then the mass magnetic susceptibility (χ , unit: 10^{-8} m³·kg⁻¹) was calculated by the formula “ $\chi = 10[(\kappa_1 + \kappa_2 + \kappa_3)/3 - (b_1 + b_2)/2]/m$ ”, and the value “ m ” is the sample mass (unit: g).

4. Results

4.1. General Characteristics and Correlations of Variations in Grain Size and Magnetic Susceptibility of Core 07SR01 Sediments

For the core 07SR01 sediments, the average of mean grain size is 4.76 Φ , ranging from 2.70 to 6.66 Φ . The sorting coefficients range from 0.55 to 3.03, with a mean of 1.71, indicating the sorting from relatively good to bad, and the samples with relatively poor sorting account for an absolute predominance. The values of skewness range from –0.20 to 0.64, with a mean of 0.26 and a relatively wide variation range. There are four skewness classes from negative to extremely positive, and the samples with positive and extremely positive skewness predominate. The values of kurtosis range from 0.69 to 2.52, with a mean of 1.14. There are four kurtosis classes from broad to very narrow, but the vast majority fall into the medium and narrow categories (Table 1). In addition, the classification of grain size for core 07SR01 sediments was carried out according to the Φ -value criterion (i.e., clay: $>8 \Phi$, silt: 4–8 Φ , and sand: $<4 \Phi$) [31]. As shown in Figure 2, the grain size composition of the whole-core sediments is dominated by silt, with contents ranging from 2.92% to 84.31% (mean: 51.75%). The clay content is the lowest, ranging from 0% to 26.24%, with a mean of 8.25%. The sand content lies in between, with a wide variation range and the highest and lowest value being 97.07% and 1.73%, respectively (mean: 40.00%). It is worth noting that the mean grain size shows a mirror-symmetric trend with the sand content and a consistent trend with the silt content, while the peaks and valleys change markedly and continuously, presuming that the dynamics for sand and silt transportation vary obviously. The variations in magnetic susceptibility are not as strong as the grain size, probably reflecting the fact that the controlled factors and environmental indications of the magnetic susceptibility variation are significantly different from those of the grain size.

The magnetic susceptibilities of core 07SR01 sediments vary from 5.8×10^{-8} to 57.3×10^{-8} m³·kg⁻¹ (mean: 27.0×10^{-8} m³·kg⁻¹) with obvious peaks and valleys, which correspond well with the content curves of the related grain size component (Figure 2). The variation curve of magnetic susceptibility shows that there is a fluctuating upward and then downward trend with several relatively small fluctuations in the drilling depth between 36.10 m and 26.65 m, ranging from 5.8×10^{-8} to 42.2×10^{-8} m³·kg⁻¹ and with a mean of 27.3×10^{-8} m³·kg⁻¹, which is similar to the whole-core average. A sudden decrease in and corresponding minimum (5.8×10^{-8} m³·kg⁻¹) of magnetic susceptibilities appears in the drilling depth of 27.07 m. The core section in the drilling depth between 26.65 m and 15.77 m is the section with the lowest magnetic susceptibilities of the whole core (variation

range: $(6.4\text{--}22.1) \times 10^{-8} \text{ m}^3 \cdot \text{kg}^{-1}$, mean: $10.6 \times 10^{-8} \text{ m}^3 \cdot \text{kg}^{-1}$). The variations in magnetic susceptibilities in this section are very small, except that a small peak and a sudden increase and corresponding maximum ($22.1 \times 10^{-8} \text{ m}^3 \cdot \text{kg}^{-1}$) appear in the drilling depth of 21.61 m and 15.92 m, respectively. The core section in the drilling depth between 15.77 m and 0 m is the section with the highest magnetic susceptibilities of the whole core (variation range: $(10.2\text{--}57.3) \times 10^{-8} \text{ m}^3 \cdot \text{kg}^{-1}$, mean: $37.4 \times 10^{-8} \text{ m}^3 \cdot \text{kg}^{-1}$). The fluctuations in magnetic susceptibilities in this section are very significant, with the largest one in the drilling depth between 3.79 m and 0.9 m.

Table 1. Grain size parameters of core 07SR01 sediments in different sections.

Depth (m)		Mean Grain Size (Φ)	Sorting Coefficient	Skewness	Kurtosis	Sample Quantity
0–36.10 (Whole core)	Minimum	2.70	0.55	−0.20	0.69	229
	Maximum	6.66	3.03	0.64	2.52	
	Mean	4.76	1.71	0.26	1.14	
26.65–36.10 (Tidal estuarine marginal bank and riverbed facies)	Minimum	2.70	0.55	0.02	0.71	65
	Maximum	5.81	2.35	0.64	2.53	
	Mean	4.02	1.56	0.35	1.32	
21.67–26.65 (Freshwater lacustrine swamp facies)	Minimum	2.83	1.51	−0.12	0.75	22
	Maximum	6.50	2.69	0.50	1.59	
	Mean	4.66	1.95	0.23	1.08	
20.50–21.67 (River floodplain facies)	Minimum	4.78	1.54	0.11	0.88	11
	Maximum	6.24	1.94	0.48	1.42	
	Mean	5.48	1.71	0.32	1.09	
15.77–20.50 (Coastal marsh facies)	Minimum	4.14	1.65	−0.15	0.70	36
	Maximum	6.55	3.03	0.53	1.24	
	Mean	5.66	1.98	0.12	0.87	
0–15.77 (Tidal estuarine delta front facies)	Minimum	2.88	0.94	−0.20	0.69	95
	Maximum	6.66	2.82	0.45	1.68	
	Mean	4.86	1.65	0.25	1.14	

In order to analyze the relationships between the magnetic susceptibilities and contents of different grain size components of core 07SR01 sediments, we divided sediment grain size into five components, i.e., clay ($>8 \Phi$), fine silt ($6\text{--}8 \Phi$), medium silt ($5\text{--}6 \Phi$), coarse silt ($4\text{--}5 \Phi$), and sand ($<4 \Phi$). And then, the correlation coefficients of the magnetic susceptibilities and contents of these five grain size components were calculated and listed in Table 2. For the core in general, the magnetic susceptibilities are positively correlated with the coarse grained components (coarse silt and sand), with a significantly better positive correlation with the sand component, suggesting that the magnetic minerals mainly occur in the coarse-grained sediments. Core 07SR01 can be divided into three sections based on the variation characteristics of magnetic susceptibilities (Figure 2), in which the lower section (26.65–36.10 m) is obviously positively correlated with the sand component, the middle section (15.77–26.65 m) is positively correlated with the coarse silt component, and the upper section (0–15.77 m) is similar to the whole section, i.e., the magnetic susceptibilities are positively correlated with the coarse-grained components (coarse silt and sand).

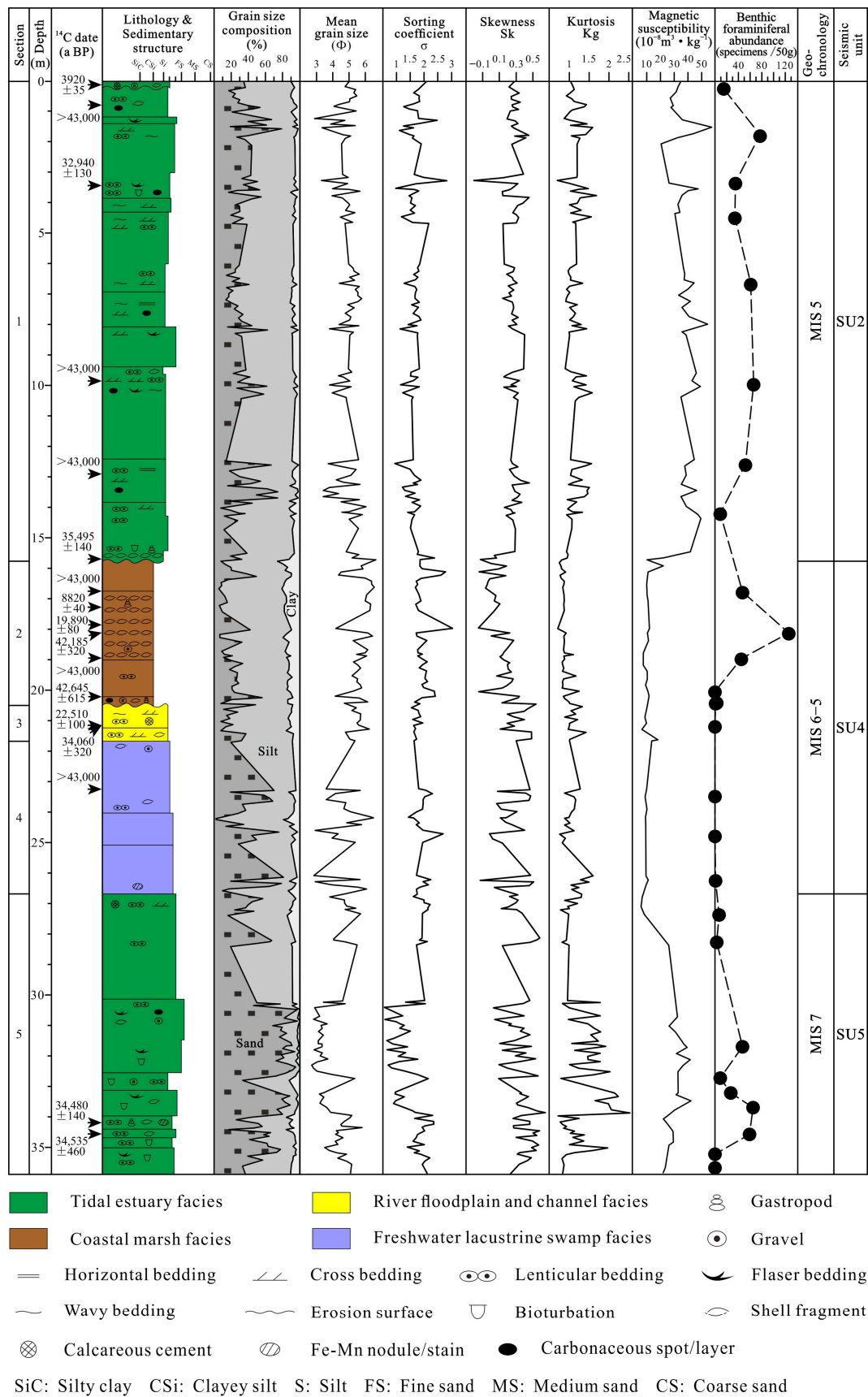


Figure 2. Integrated column of core 07SR01 sediments (modified after reference [33]).

Table 2. Correlation coefficients between grain size and magnetic susceptibility of core 07SR01 sediments in different sections.

Core Section (Depth or Sedimentary Facies)	Grain Size (Φ)				
	>8	6–8	5–6	4–5	<4
0–36.10 m	−0.544 **	−0.407 **	−0.207 *	0.126	0.280 **
26.65–36.10 m	−0.600 **	−0.514 **	−0.633 **	−0.817 **	0.712 **
15.77–26.65 m	0.018	−0.024	−0.025	0.145 *	−0.030
0–15.77 m	−0.500 **	−0.304 *	−0.087	0.118	0.254 *
Tidal estuarine marginal bank and riverbed facies	−0.600 **	−0.514 **	−0.633 **	−0.817 **	0.712 **
Freshwater lacustrine swamp facies	0.084	0.141 *	0.187 *	0.164 *	−0.163 *
River floodplain facies	−0.935 **	−0.690 **	−0.028	0.620 **	0.581 **
Coastal marsh facies	−0.058	−0.112 *	−0.177 *	0.066	0.109
Tidal estuarine delta front facies	−0.500 **	−0.304 *	−0.087	0.118	0.254 *

Notes: The correlation coefficients marked “*” and “**” have passed the significance test on the level of $p < 0.05$ and $p < 0.01$, respectively.

4.2. Characteristics and Correlations of Variations in Grain Size and Magnetic Susceptibility of Core 07SR01 Sediments in Different Sedimentary Facies

Xia et al. [28,29,33,34] conducted some detailed analyses and delineations of sedimentary facies of core 07SR01 based on the results of sediment component, color, sedimentary texture and structure, macro- and micro-fossils, and other indicators. Based on the previous understanding, this paper revisited the identification and delineation of the sedimentary facies of core 07SR01 and revised and improved them, combining them with the characteristics of vertical variations of magnetic susceptibility and grain size and the interpretation results of cores and shallow seismic profiles for the estuarine delta facies [35–38]. With the exception of core Section 1, this paper’s understanding of the sedimentary facies of the rest of the core sections (Sections 2–5) is consistent with that of the previous authors [33,34]. The sedimentary and seismic characteristics of Section 1 (abundant tidal beddings; a complex alternation of clinofolds; and chaotic to hummocky reflections with cut-and-fill geometries; see reference [33,34] for details) are consistent with those of the typical tidal estuarine delta front identified in the cores and shallow seismic profiles of other regions (Figures 3–5, see Figure 1 for the locations of track lines). Meanwhile, the analysis results show that variations in the magnetic susceptibility and grain size of sediments in this section correspond well with the sediment dynamics of the estuarine area (see Section 5.2 below for details). Therefore, the revised sedimentary facies sequence of core 07SR01 (Figure 2) is as follows: tidal estuarine delta front facies (0–15.77 m), coastal marsh facies (15.77–20.50 m), river floodplain facies (20.50–21.67 m), freshwater lacustrine swamp facies (21.67–26.65 m), and tidal estuarine marginal bank and riverbed facies (26.65–36.10 m).

The variation characteristics of grain size parameters and magnetic susceptibilities and grain size frequency distribution curves in different sedimentary facies are shown in Figures 2 and 6 and Table 1, and it can be found that there are variations in each parameter and grain size frequency distribution curve for different sedimentary facies with obvious differences. In addition, the magnetic susceptibility has different variation mechanisms and various correlations with sediment grain size in different regions and sedimentary environments [39]. Therefore, the correlation coefficients of magnetic susceptibility and grain size in the different sedimentary facies of core 07SR01 are calculated and listed in Table 2. The variation characteristics of each parameter and the frequency distribution curves of grain size and the correlations between magnetic susceptibility and grain size in different sedimentary facies are specified as follows.

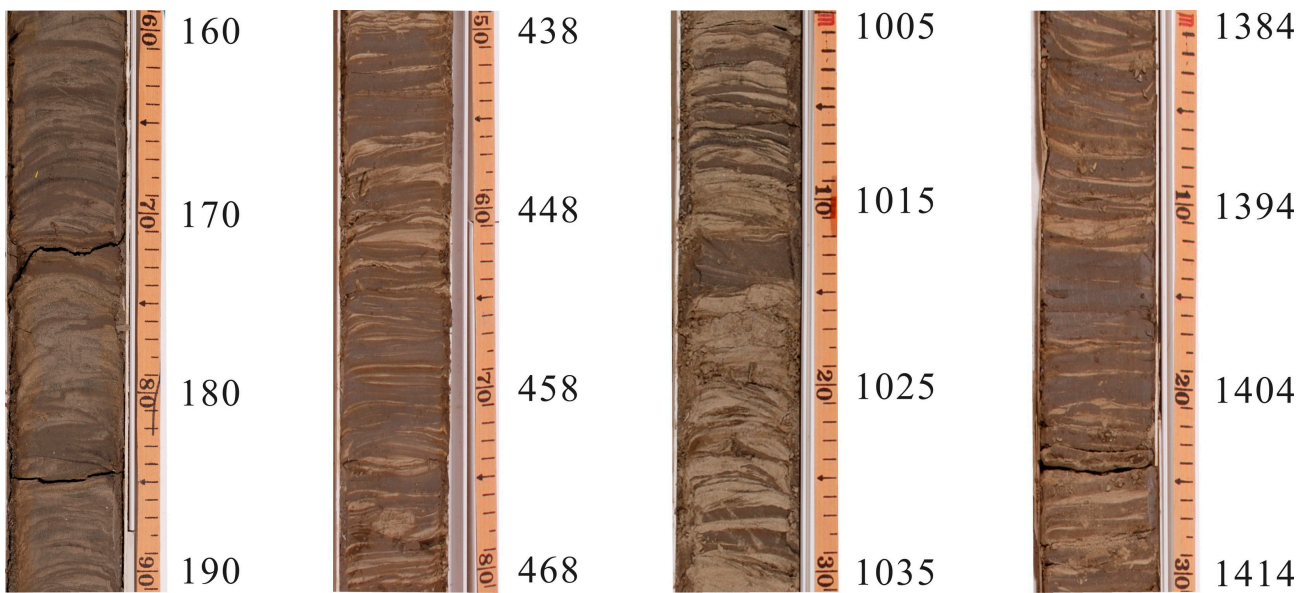


Figure 3. Photos of Section 1 of core 07SR01 sediments showing the typical sedimentary structures of tidal estuarine delta front; the numbers in the figure indicate the core drilling depth (unit: cm).

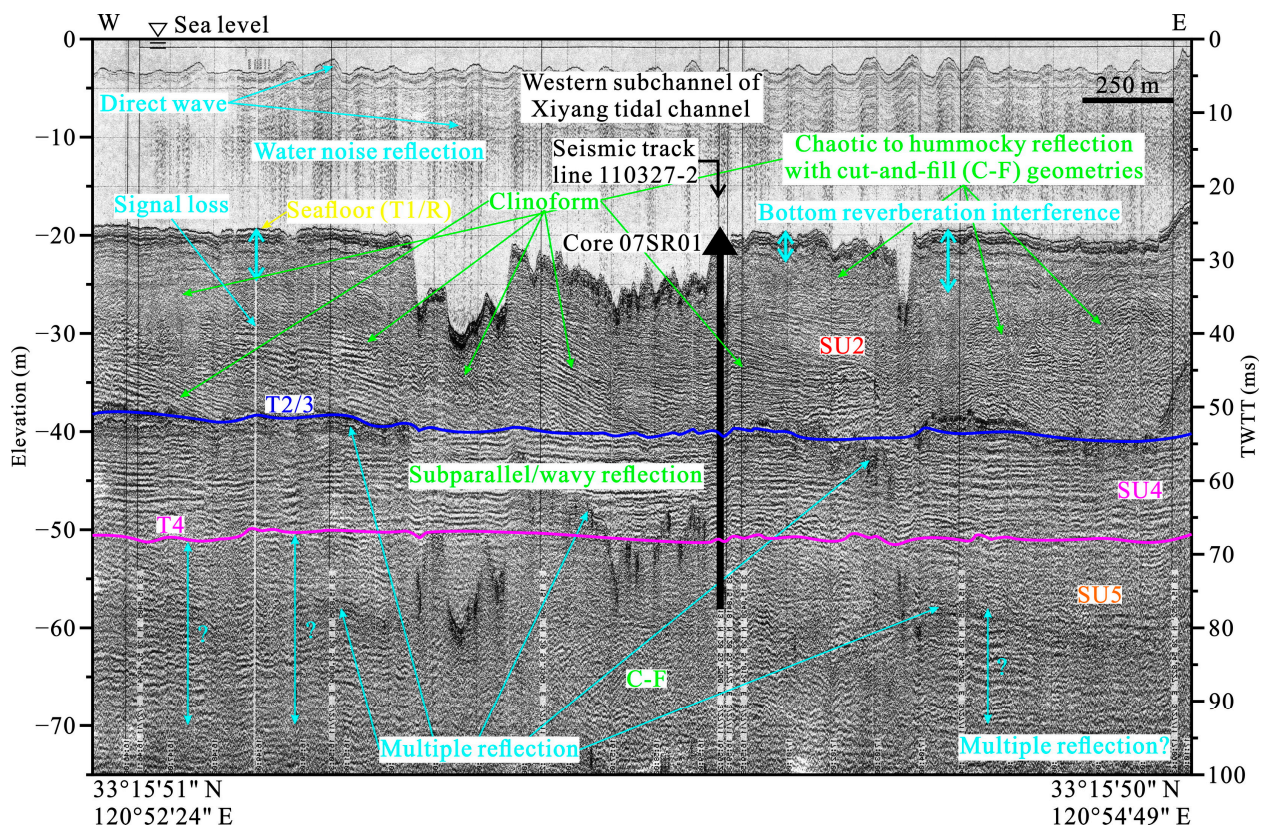


Figure 4. Shallow seismic profile of track line 110327-4-2 in the Xiyang tidal channel and its interpretations; the original seismic data were acquired by the authors of this paper in March 2011 using a GeoPulse sub-bottom profiler (GeoAcoustics Ltd., Great Yarmouth, UK), and they were also interpreted by the authors of this paper; the capital letters SU show the seismic units, and the capital letter T shows the seismic bounding surfaces; two-way travel times (TWTT) from the seismic profile were converted to sediment thicknesses using an acoustic velocity of 1500 m/s.

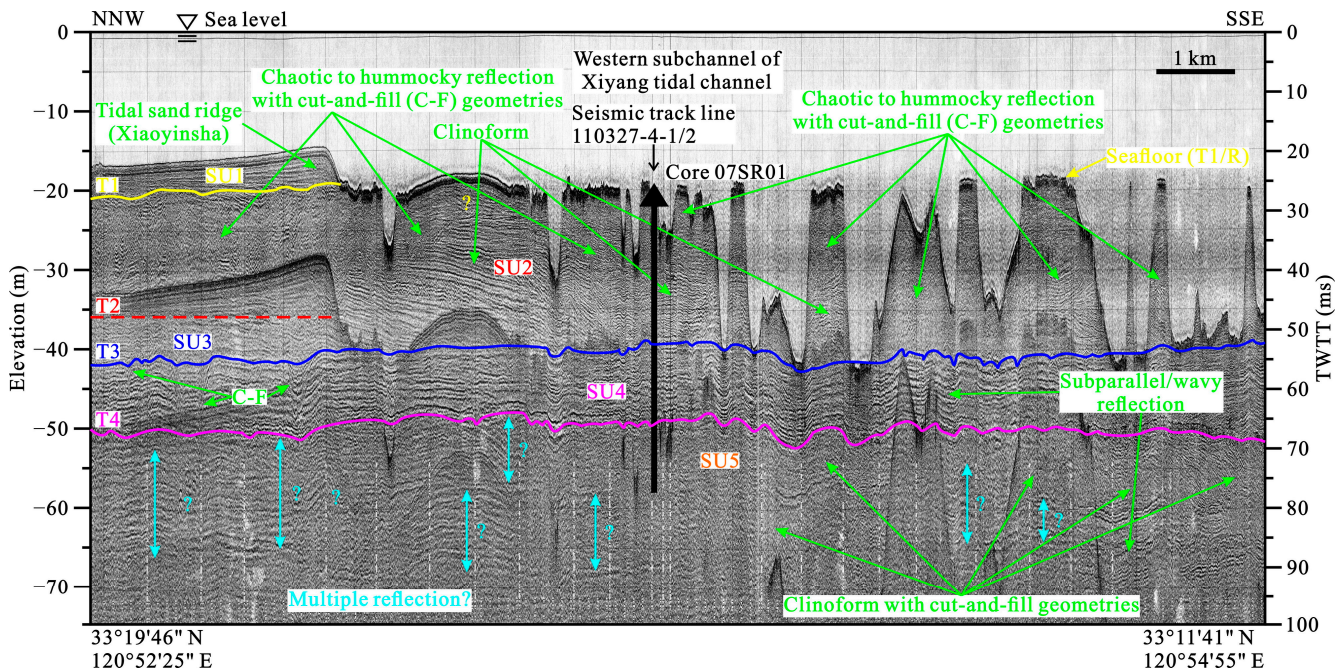


Figure 5. Shallow seismic profile of track line 110327-2 in the Xiyang tidal channel and its interpretations; the original seismic data were acquired by the authors of this paper in March 2011 using a GeoPulse sub-bottom profiler (GeoAcoustics Ltd., Great Yarmouth, UK), and they were also interpreted by the authors of this paper; the capital letters SU show the seismic units and the capital letter T shows the seismic bounding surfaces; two-way travel times (TWT) from the seismic profile were converted to sediment thicknesses using an acoustic velocity of 1500 m/s.

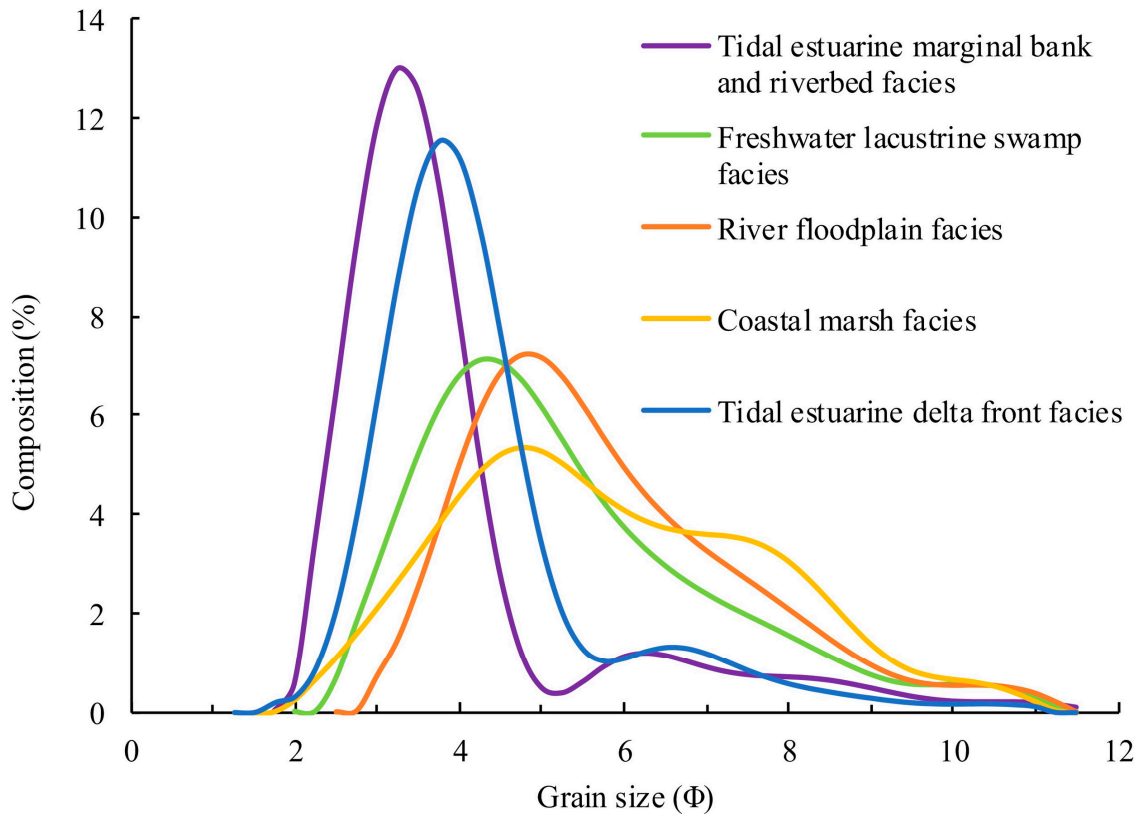


Figure 6. Grain size frequency distribution curves of representative samples from sections of core 07SR01 with different sedimentary facies.

4.2.1. Tidal Estuarine Marginal Bank and Riverbed Facies (Section 5, 26.65–36.10 m)

The sediments are relatively coarse and mainly composed of sands, with the mean grain size ranging from 2.70 to 5.81 Φ (mean: 4.02 Φ), which are the smallest Φ -values in the whole core. The sorting ranges from relatively good to poor (sorting coefficients ranging from 0.55 to 2.35, with a mean of 1.56). The skewness ranges from nearly symmetric to extremely positive skewness (the values of skewness ranging from 0.02 to 0.64, with a mean of 0.35), and most of the samples exhibit extremely positive skewness. The kurtosis is from broad to very narrow (the values of kurtosis range from 0.71 to 2.53, with a mean of 1.32 which belongs to a narrow peak). The frequency distribution curves show that the main peak with extremely positive skewness is prominent and located near 3 Φ , with a secondary peak or thin tail appearing near 6 Φ . The magnetic susceptibilities are relatively high, ranging from 5.81×10^{-8} to $42.16 \times 10^{-8} \text{ m}^3 \cdot \text{kg}^{-1}$ (mean: $27.06 \times 10^{-8} \text{ m}^3 \cdot \text{kg}^{-1}$), which are strongly and positively correlated with the grain size component of <4 Φ (correlation coefficient: 0.712).

4.2.2. Freshwater Lacustrine Swamp Facies (Section 4, 21.67–26.65 m)

The sediment grain sizes vary widely and show a decrease in sand content and an increase in silt and clay content, with the mean grain size ranging from 2.83 to 6.50 Φ (mean: 4.66 Φ). The sorting ranges from relatively poor to poor (the sorting coefficients range from 1.51 to 2.69, with a mean of 1.95). The skewness varies in a wide range, from negative to extremely positive (the values of skewness ranging from -0.12 to 0.50, with a mean of 0.23), and the vast majority of samples exhibited positive skewness. The kurtosis ranges from wide to very narrow (the values of kurtosis range from 0.75 to 1.59, with a mean of 1.08 which belongs to a medium peak). The frequency distribution curves show that a single main peak with positive skewness is located near 4.25 Φ . The magnetic susceptibilities are weakly and positively correlated with the grain size component of >4 Φ (correlation coefficient: 0–0.2), which is related to the reduction in coarse-grained components in sedimentary environments. The magnetic susceptibilities of this section are the lowest among all sedimentary facies and have the smoothest variation trend, ranging from 8.79×10^{-8} to $11.08 \times 10^{-8} \text{ m}^3 \cdot \text{kg}^{-1}$ (mean: $9.65 \times 10^{-8} \text{ m}^3 \cdot \text{kg}^{-1}$).

4.2.3. River Floodplain Facies (Section 3, 20.50–21.67 m)

The sediments become finer and are dominated by silt, showing a decrease in sand content and an increase in clay and silt content, with the mean grain size ranging from 4.78 to 6.24 Φ (mean: 5.48 Φ). The sorting ranges relatively poor (sorting coefficients ranging from 1.54 to 1.94, with a mean of 1.71). The skewness ranges from nearly symmetric to extremely positive (the values of skewness ranging from 0.11 to 0.48, with a mean of 0.32), with positive skewness predominating. The kurtosis ranges from wide to very narrow (the values of kurtosis range from 0.88 to 1.42, with a mean of 1.09 which belongs to a medium peak). The frequency distribution curves show that a single main peak with positive skewness is located near 4.75 Φ . The magnetic susceptibilities are relatively low, ranging from 6.46×10^{-8} to $19.39 \times 10^{-8} \text{ m}^3 \cdot \text{kg}^{-1}$ (mean: $12.04 \times 10^{-8} \text{ m}^3 \cdot \text{kg}^{-1}$), which are strongly and positively correlated with the grain size component of <5 Φ (correlation coefficient: ~ 0.6).

4.2.4. Coastal Marsh Facies (Section 2, 15.77–20.50 m)

The sediments are still dominated by silt, showing a decrease in sand content and an increase in clay and silt content, with the mean grain size ranging from 4.14 to 6.55 Φ (mean: 5.66 Φ). The sorting is from relatively poor to poor (sorting coefficients ranging from 1.65 to 3.03, with a mean of 1.98). The skewness varies in a wide range, from negative to extremely positive (the values of skewness ranging from -0.15 to 0.53, with a mean of 0.12), with positive skewness predominating. The kurtosis is from wide to narrow (the values of kurtosis ranging from 0.70 to 1.24, with a mean of 0.87 which belongs to a broad peak). The frequency distribution curves show that a single main peak with positive skewness

is located near 4.75Φ , and there is an obvious inflection point near 8Φ . The magnetic susceptibilities are relatively low, ranging from 7.46×10^{-8} to $20.04 \times 10^{-8} \text{ m}^3 \cdot \text{kg}^{-1}$ (mean: $10.79 \times 10^{-8} \text{ m}^3 \cdot \text{kg}^{-1}$), which are weakly and positively correlated with the grain size component of $<5 \Phi$ (correlation coefficient: ~ 0.1).

4.2.5. Tidal Estuarine Delta Front Facies (Section 1, 0–15.77 m)

The sediments become coarser, showing an increase in sand content and a decrease in clay and silt content, with the mean grain size ranging from 2.88 to 6.66 Φ (mean: 4.86 Φ). The sorting is from moderate to poor (sorting coefficients ranging from 0.94 to 2.82, with a mean of 1.65). The skewness varies in a wide range, from negative to extremely positive (the values of skewness ranging from -0.20 to 0.45 , with a mean of 0.25). The kurtosis is from broad to very narrow (the values of kurtosis ranging from 0.69 to 1.68 , with a mean of 1.14 which belongs to a narrow peak). The frequency distribution curves are similar to those of Section 5, with a prominent main peak located near 3.75Φ and a secondary peak or thin tail appearing near 6.5Φ . The magnetic susceptibilities of this section are the highest among all sedimentary facies and have the most volatile variation trend, ranging from 10.21×10^{-8} to $57.25 \times 10^{-8} \text{ m}^3 \cdot \text{kg}^{-1}$ (mean: $37.15 \times 10^{-8} \text{ m}^3 \cdot \text{kg}^{-1}$), which are weakly and positively correlated with the grain size component of $<5 \Phi$ (correlation coefficient: $0.1\text{--}0.3$).

5. Discussion

5.1. Chronological Framework of Core 07SR01 Sediments

More than a decade ago, Xia et al. [28,29,33] put forward a chronological framework of core 07SR01 sediments based on four selected “reliable” AMS ^{14}C dates and the curve of global sea level changes. The results show that from top to bottom, the first stiff mud layer of continental facies (Sections 3 and 4) should be formed in MIS 2, and the coastal marsh deposits (Section 2) which overlay on the first stiff mud layer correspond to the transgression boundary layer of MIS 1 [28,29,33]. Accordingly, Sections 1 and 5 (original interpretation: tidal sand ridge and channel, coastal barrier island, respectively) should be formed in MIS 1 and MIS 3, respectively [28,29,33]. In recent years, Xia et al. [34] rethought the shallow sedimentary sequence and its evolution of the Xiyang tidal channel in the RSRF. The results show that the chronological framework of core 07SR01 sediments established by previous studies is erroneous, and the second stiff mud layer (Sections 3 and 4, which may be formed in MIS 4 or earlier) was mistakenly treated as the first stiff mud layer (which should be formed in MIS 2). Furthermore, the main body of core 07SR01 should be the Late Pleistocene deposits, and the first stiff mud layer is mostly missing because of the strong tidal current erosion [34]. Accordingly, Sections 1, 2, and 5 should be formed in MIS 3, MIS 3, and MIS 5, respectively [34].

In this paper, based on the existing understandings of the shallow sedimentary sequence and age of the Xiyang tidal channel, we completed further correlations of the shallow sedimentary sequences and ages of key cores in the Xiyang tidal channel and its adjacent area on the northwest side (Figure 7, see Figure 1 for the locations of the cores) and reconstructed again the chronological framework of core 07SR01 sediments as follows: Section 5 (36.10–26.65 m): MIS 7, Sections 4–2 (26.65–15.77 m): MIS 6–5, and Section 1 (15.77–0 m): MIS 5 (Figures 2 and 7). In addition, the topmost part of Section 1 (0–0.12 m) was attributed to the modern tidal channel lag deposits. This age inference was based on four aspects as follows: (1) More recent studies show that the ^{14}C dating technique has an obvious limitation regarding the dating of relatively old (>30 ka BP) samples and may significantly underestimate the ages of sediments for samples older than 30 ka BP because of the contamination of young carbons [40–45]. Consequently, the general inversion and disorder of the AMS ^{14}C dates of core 07SR01 sediments may be caused by sediment erosion–re-deposition and contamination under the strong tidal sediment dynamics. Moreover, the majority of the AMS ^{14}C dates are >30 ka BP or exceed the upper limit of AMS ^{14}C dating and therefore have large errors and are not suitable for direct

adoption. (2) In the section corresponding to Section 1, all the ^{14}C dates (sixteen) of these cores range from ca. 30 to >43.5 ka BP, except for three dates, while all the quartz OSL dates (six) range from ca. 60 to ca. 100 ka except for one date, and half of them have saturated OSL signals (equivalent dose (D_e) >200 Gy, the same below), indicating probable age underestimations [33,46–48]. (3) In the section corresponding to Sections 2–4, all the ^{14}C dates (twelve) of these cores range from ca. 34 to >43.5 ka BP, except for three dates, while one quartz OSL date is 94.7 ± 8.5 ka with saturated OSL signals, also indicating probable age underestimations [33,47,48]. (4) In the section corresponding to Section 5, core 07SR01 yields two AMS ^{14}C dates which are both >34 ka BP, core JC-1202 yields three quartz OSL dates ranging from 144 to 211 ka, and core JSWZK03 yields five dates, with the quartz OSL dates (four) ranging from >134.2 to >170 ka and the AMS ^{14}C date greater than 43.5 ka BP [33,47,48]. Moreover, the quartz OSL signals in all samples of this section are saturated, indicating that these dates are presumably underestimated. On the basis of the above four aspects, it can be further inferred that in core 07SR01, the strata of the first continental facies and marine facies formed in MIS 4–2 and MIS 1, respectively, are missing because of both the strong tidal current scouring and anthropogenic activities.

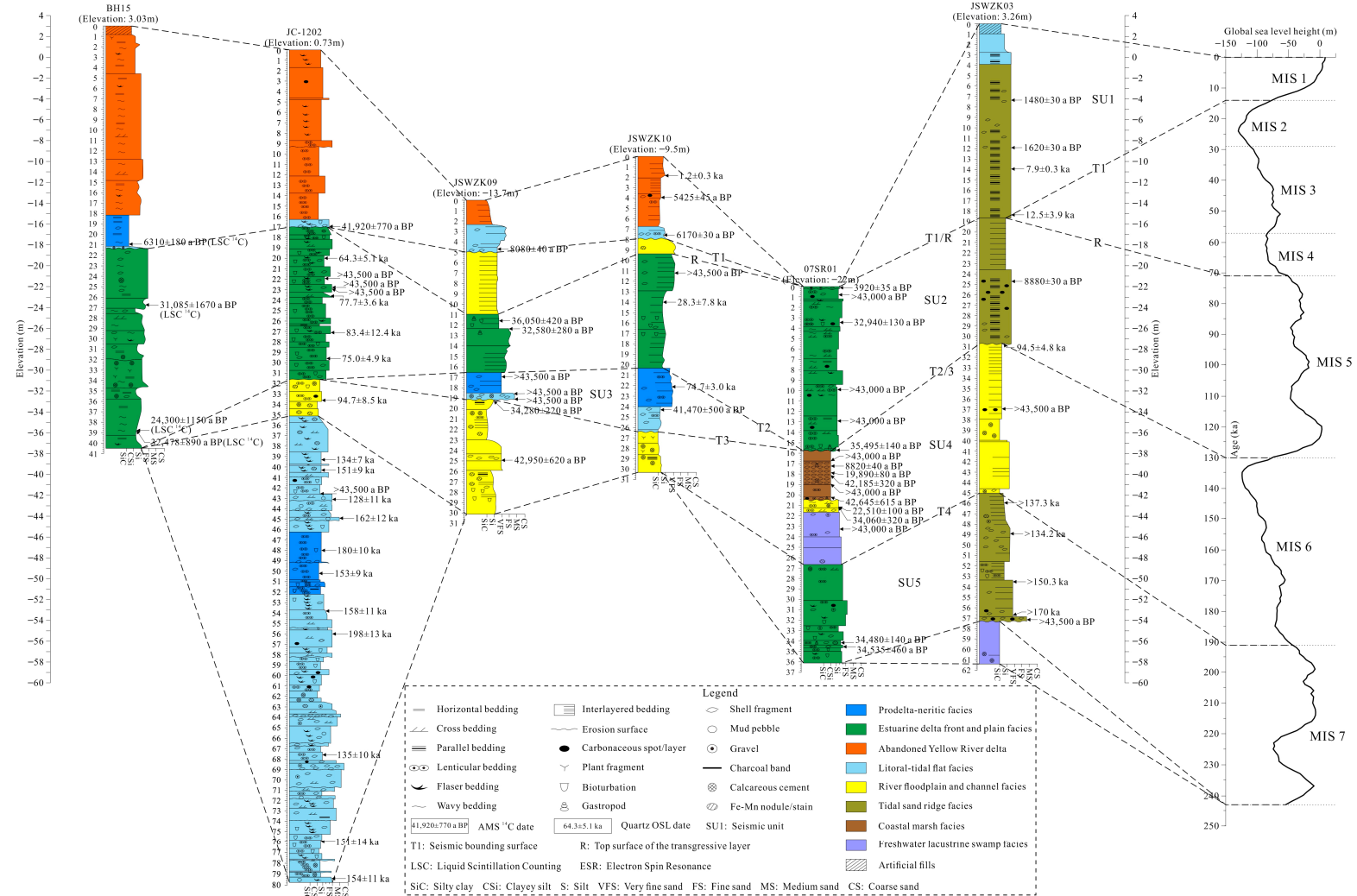


Figure 7. Correlation of the Late Quaternary sedimentary sequences of mainly studied cores in the Xiyang tidal channel and its adjacent area on the northwest side; core 07SR01 was modified after reference [33]; core BH15 was modified after reference [46]; core JC-1202 was modified after reference [47]; core JSWZK03, JSWZK09, and JSWZK10 were modified after reference [48]; the curve of global sea level changes was modified after reference [49].

5.2. Environmental Indications for Combination of Grain Size and Magnetic Susceptibility of Core 07SR01 Sediments and Corresponding Regional Sedimentary Evolution

Variations in the grain size and magnetic susceptibility of sediments in the river–sea interaction area could indicate environmental changes [4–9,12–16,50]. In addition, the above analyses show that the grain size and magnetic susceptibility of core 07SR01 sediments responded well to the changes in sedimentary environments. Therefore, combining this with the reinterpretation results of the sedimentary sequence and age of core 07SR01 and shallow seismic profiles, as well as the findings of the climate and glacial–eustatic cycles of the Northern Hemisphere during Late Quaternary [49,51], the environmental indications for the combination of the grain size and magnetic susceptibility of core 07SR01 sediments and the corresponding sedimentary evolution of the Xiyang tidal channel between MIS 7 and MIS 5 can be divided into the following three stages.

5.2.1. Stage 1 (MIS 7, Section 5: 36.10–26.65 m)

The sediments deposited in this stage are coarse and dominated by sand with regard to grain size composition, while the content of silt and clay is very low. The fluctuations in sorting, skewness, and kurtosis are large, and the frequency distribution curves exhibit a narrow peak with extremely positive skewness, dragging a thin tail, which reflects the strong hydrodynamic conditions and tidal current influence [52]. The magnetic susceptibilities are relatively high and significantly fluctuating, which is related to the fact that the magnetic minerals are mainly enriched in the coarse-grained components and is further indicative of the tidal estuarine marginal bank and river bed environments under the high sea level and the influence of relatively strong hydrodynamics during the warm period of MIS 7. The results of previous studies show that the Changjiang River-derived sediments are relatively coarse in grain size and relatively high in magnetic susceptibility, and the magnetic minerals are mainly enriched in the coarse-grained sediments [12,13,20]. The characteristics of the grain size and magnetic susceptibility of core 07SR01 sediments in this stage are similar to the above-mentioned features. Meanwhile, the contents of carbonate minerals (i.e., dolomite, vaterite, and calcite, which could serve as a proxy of the Yellow River's impact) in this stage are relatively low [33]. Moreover, the study area was located in the estuarine area of the paleo-Changjiang River at that time [53]. Consequently, it is assumed that the study area was mainly affected by the paleo-Changjiang River-derived sediments in this stage.

5.2.2. Stage 2 (MIS 6–5, Sections 4–2: 26.65–15.77 m)

Based on the variation characteristics of the magnetic susceptibility and grain size of sediments and the sedimentary facies, this stage can be further subdivided into Stage 2-1 (26.65–20.50 m) and Stage 2-2 (20.50–15.77 m). In Stage 2-1, the grain size composition of sediments was refined, and the content of sand and silt decreased and increased sharply, respectively, while the content variations in clay were not obvious. The fluctuations in sorting became smaller, the skewness changed from extremely positive to positive, and the kurtosis became wider. The magnetic susceptibility stayed at a low level and its variations were quite smooth, with the lowest values in the whole core, and this was related to the reduction in coarse sediment input in sedimentary environments, indicating that the hydrodynamic conditions in this stage were weakened and stabilized compared with those in Stage 1, and both the sea level and air temperature decreased, corresponding to the environments of freshwater lacustrine swamp and river floodplain in the context of the cold–dry climate and sea level fall in MIS 6. The sediments in Stage 2-2 continued to become finer, and the content of sand and silt continued to decrease and increase, respectively, while the content of clay increased significantly. The sorting fluctuated significantly once again, and the characteristics of double skewness predominated by positive skewness reflect the alternate deposition of coarse and fine sediment components in the context of enhanced hydrodynamic conditions. The inflection point at the fine-grained end of the frequency distribution curve is obvious, which is probably due to the changes in

sedimentary dynamic processes and the influence of seawater [4,6]. In addition, the magnetic susceptibility, although still at a low level, began to fluctuate, which further indicates that the hydrodynamic conditions in Stage 2-2 were enhanced compared with those in Stage 2-1, and the sea level and air temperature increased, corresponding to the coastal marsh environments in the context of the transition from MIS 6 to MIS 5 and the marine transgression of MIS 5. Overall, the sediments in Stage 2 became finer, with slightly poorer but more stable sorting, predominantly positive skewness, and broader kurtosis. Moreover, the frequency distribution curves showed the broad peak with positive skewness moving toward the fine-grained end, and the magnetic susceptibilities were relatively low and stable. All of these were indicative of the low-energy, stable and low-sea-level environments, in which both the oxidability and reducibility were once relatively strong, dominated by the deposits of terrestrial and coastal marsh facies, corresponding to the period of MIS 6–5 that changed from cold–dry to warm–moist climatic conditions, with a falling sea level followed by a rising sea level. In addition, this stage was characterized by the one-time reductive environments with long-lasting stagnant water, and Fe-Mn nodules were found in the corresponding layers, which is one of the indicators of early diagenesis [54]. The early diagenesis of sediments under reductive conditions leads to the dissolution of and phase change in magnetic minerals. Moreover, this process is closely related to the content of organic matter in sediments because the decomposition of organic matter will consume the dissolved oxygen in the water body and form a reductive environment, which will prompt the dissolution of iron-containing minerals and reduce the content of magnetic minerals, resulting in lower magnetic susceptibilities [22–24]. Therefore, it is assumed that the lower magnetic susceptibilities in this stage may be related to the early diagenesis of sediments to a certain extent.

5.2.3. Stage 3 (MIS 5, Section 1: 15.77–0 m)

Compared with the previous stage, the mean grain size of sediments in this stage increased, while the content of sand increased rapidly, and the content of silt and clay decreased. The fluctuations in sorting were obvious, and its variation range became larger. The frequency distribution curves showed a narrow peak with extremely positive skewness moving toward the coarse grained end and dragging a thin tail, and the kurtosis became narrower. The magnetic susceptibilities increased rapidly and fluctuated frequently with a large range, reflecting the complexity of interactions between the rising sea level and various strong hydrodynamics in the estuary. The sedimentary structure was also characterized by a specific type of tidal rhythmites with the sand–mud–interlayered bedding (Figure 3), which corresponded to the tidal estuarine delta front environments under the background of the fluctuating sea level rise in the warm period of MIS 5. In addition, compared with Stage 1, which was also characterized by high and fluctuating magnetic susceptibilities, the input of coarse-grained sediments was reduced (the sand content was lower than that in Stage 1), and the positive correlations between magnetic susceptibilities and coarse-grained components became weaker, probably indicating that the sediment provenance in this stage changed compared with that in Stage 1. Meanwhile, the contents of carbonate minerals in eight samples above the drilling depth of 16.14 m showed an obvious increase, indicating the enhanced impact of the paleo-Yellow River-derived sediments [33]. The core NTCJ1 in the Sheyang estuary also recorded a delta front deposit in the MIS 5 tidal estuary, which was obviously influenced by the paleo-Yellow River [55]. Accordingly, during this period, the Changjiang River probably migrated southward and gradually moved away from the study area. Meanwhile, the input of its sediments to the north was limited, while the Yellow River presumably flowed into the South Yellow Sea through the northern Jiangsu, and the study area was under the increased impact of the paleo-Yellow River-derived sediments of MIS 5 in the case of the littoral currents carrying the Yellow River sediments to the south.

6. Conclusions

The grain size and magnetic susceptibility of core 07SR01 sediments responded well to changes in sedimentary environments and were indicative of the environments to a certain extent. Combining this with the reinterpretation results of the sedimentary sequence and age of this core and shallow seismic profiles, as well as the findings of the climate and glacial–eustatic cycles of the Northern Hemisphere during Late Quaternary, the characteristics and environmental indications for the combination of grain size and magnetic susceptibility of core 07SR01 sediments and the corresponding sedimentary evolution of the Xiyang tidal channel between MIS 7 and MIS 5 can be revealed and summarized in three stages as follows:

Stage 1: This stage entails marginal bank and riverbed developments in the tidal estuary under a relatively high sea level and strong hydrodynamic conditions during MIS 7 (core section: 36.10–26.65 m). The sediments deposited in this stage were mainly affected by the paleo-Changjiang River and were characterized by a coarse grain size (mean: 4.02 Φ), dramatic fluctuations in relatively good sorting, extremely positive skewness with a high–narrow peak near 3 Φ and a thin tail in the frequency distribution curve, and relatively high magnetic susceptibilities (mean: $27.06 \times 10^{-8} \text{ m}^3 \cdot \text{kg}^{-1}$) with small fluctuations which were strongly and positively correlated with the sand component (<4 Φ).

Stage 2: This is the stage dominated by fluviolacustrine and littoral environments, with weak hydrodynamics during MIS 6–5, in which the climate changed from cold and dry to warm and humid as the sea level rose after a drop (core section: 26.65–15.77 m). The sediments deposited in this stage were characterized by a fine grain size (mean: 5.27 Φ), relatively small variations in poor sorting, except for the uppermost part, positive skewness with a low–broad peak near 4.75 Φ in the frequency distribution curve, and low magnetic susceptibilities with minor variations (mean: $10.83 \times 10^{-8} \text{ m}^3 \cdot \text{kg}^{-1}$) which were weakly and positively correlated with the coarse silt component (4–5 Φ).

Stage 3: This stage concerns the delta front in the tidal estuary with a relatively high sea level and strong hydrodynamics during MIS 5 (core section: 15.77–0 m). The sediments deposited in this stage were strongly influenced by the paleo-Yellow River and characterized by a relatively coarse grain size (mean: 4.86 Φ), relatively small variations in medium to relatively poor sorting except for the uppermost part, extremely positive skewness with a high–narrow peak near 3.75 Φ and a thin tail in the frequency distribution curve, and high magnetic susceptibilities (mean: $37.15 \times 10^{-8} \text{ m}^3 \cdot \text{kg}^{-1}$) with large fluctuations which were weakly and positively correlated with the sand and coarse silt components (<5 Φ).

Author Contributions: Conceptualization, F.X. and D.L.; methodology, F.X.; software, D.L.; validation, F.X., D.L. and Y.Z.; formal analysis, F.X.; investigation, F.X.; resources, F.X. and Y.Z.; data curation, F.X.; writing—original draft preparation, F.X. and D.L.; writing—review and editing, F.X.; visualization, F.X. and D.L.; supervision, Y.Z.; project administration, F.X.; funding acquisition, F.X. and Y.Z. All authors have read and agreed to the published version of the manuscript.

Funding: This research was funded by the National Natural Science Foundation of China (Grant No. 41901107), the Natural Science Foundation of the Jiangsu Higher Education Institutions of China (Grant No. 18KJB170003), and the Scientific Research Start-Up Foundation for the Introduced High-Level Talents of Jiangsu Second Normal University (Grant No. 919801).

Institutional Review Board Statement: Not applicable.

Informed Consent Statement: Not applicable.

Data Availability Statement: Data will be made available on request.

Acknowledgments: This is a major revision and translation of “Characteristics of grain size and magnetic susceptibility of the Late Quaternary sediments from core 07SR01 in the middle Jiangsu coast and their paleoenvironmental significances” originally published in Chinese by “Marine Geology & Quaternary Geology, 2021, 41(5), 210–220”. This major revision and translation was prepared by Fei Xia, Dezheng Liu, and Yongzhan Zhang with support from National Natural Science Foundation of China. Permission was granted by the Editorial Office of Marine Geology & Quaternary Geology.

The authors are very grateful to Ying Wang and Shu Gao of Nanjing University and Jian Wang of Jiangsu Second Normal University for their important support and mentoring, to Gang Li, Zhuyou Sun, and Ning Zhang of Nanjing University for their participation in the field drilling and laboratory experiment, and to the three anonymous reviewers for their constructive comments.

Conflicts of Interest: The authors declare no conflicts of interest.

References

- Prins, M.A.; Postma, G.; Weltje, G.J. Controls on terrigenous sediment supply to the Arabian Sea during the late Quaternary: The Makran continental slope. *Mar. Geol.* **2000**, *169*, 351–371. [[CrossRef](#)]
- Shu, Q.; Li, C.L.; Zhao, Z.J.; Chen, Y.; Zhang, M.H.; Li, J.J. The records of mass susceptibility and grain size for climate changes in Subei Basin during the last deglaciation. *Acta Sediment. Sin.* **2009**, *27*, 111–117. (In Chinese with English abstract)
- Cai, T.L.; Jia, J.J.; Wang, Y.P. Techniques for particle size data standardization: An example from estuarine and coastal sediments. *Mar. Geol. Quat. Geol.* **2014**, *34*, 185–193. (In Chinese with English abstract)
- Deng, C.W.; Zhang, X.; Lin, C.M.; Yu, J.; Wang, H.; Yin, Y. Grain-size characteristics and hydrodynamic conditions of the Changjiang estuarine deposits since last glacial. *Mar. Geol. Quat. Geol.* **2016**, *36*, 185–198. (In Chinese with English abstract)
- Wang, Z.B.; Yang, S.Y.; Zhang, Z.X.; Li, R.H.; Wang, H.; Lan, X.H. The grain size compositions of the surface sediments in the East China Sea: Indication for sedimentary environments. *Oceanol. Limnol. Sin.* **2012**, *43*, 1039–1049. (In Chinese with English abstract)
- Ding, D.L.; Zhang, X.H.; YU, J.J.; Wang, L.Y.; Wang, F.; Shang, S.W. Sediment grain size distribution patterns of the late Quaternary on the back side of northern Yangtze River Delta and their environmental implications. *Mar. Geol. Quat. Geol.* **2019**, *39*, 34–45. (In Chinese with English abstract)
- Zhou, L.C.; Li, J.; Gao, J.H.; Bai, F.L.; Zhao, J.T. Comparison of core sediment grain-size characteristics between Yangtze River estuary and Zhoushan Islands and its significance to sediment source analysis. *Mar. Geol. Quat. Geol.* **2009**, *29*, 21–27. (In Chinese with English abstract)
- Li, H.J.; Liu, Y.; Cheng, Y.; Zhang, C.P.; Gao, J.H.; Liu, J.W.; Zhang, L.; Zheng, J.H. Characteristics of sediment grain size at Yalu River estuary and implications for depositional environment. *Mar. Geol. Quat. Geol.* **2017**, *37*, 58–66. (In Chinese with English abstract)
- Pan, F.; Lin, C.M.; Li, Y.L.; Zhang, X.; Zhou, J.; Qu, C.W.; Yao, Y.L. Sediments grain-size characteristics and environmental evolution of Core SE2 in southern bank of Qiantang River since the Late Quaternary. *J. Palaeogeogr.* **2011**, *13*, 236–244. (In Chinese with English abstract)
- Thompson, R.; Oldfield, F. *Environmental Magnetism*; Allen & Unwin: London, UK, 1986; pp. 1–227.
- Verosub, K.L.; Roberts, A.P. Environmental magnetism: Past, present, and future. *J. Geophys. Res. Solid Earth* **1995**, *100*, 2175–2192. [[CrossRef](#)]
- Jia, H.L.; Liu, C.Z.; Zhang, W.G.; Meng, Y.; Hong, X.Q. Magnetic properties of core CY from Chongming island, the Yangtze estuary and its environmental significance. *Acta Sediment. Sin.* **2004**, *22*, 117–123. (In Chinese with English abstract)
- Zhang, R.H.; Xie, J.L.; Liu, T.; Zhao, B.C. Palaeoenvironmental evolution of subaqueous Yangtze delta inferred from sedimentary records. *Mar. Geol. Quat. Geol.* **2011**, *31*, 1–10. (In Chinese with English abstract) [[CrossRef](#)]
- Ge, Z.S. Study on magnetic susceptibility of hole QC₂ in the South Yellow Sea. *Mar. Geol. Quat. Geol.* **1996**, *16*, 35–42. (In Chinese with English abstract)
- Yim, W.W.-S.; Huang, G.; Chan, L.S. Magnetic susceptibility study of Late Quaternary inner continental shelf sediments in the Hong Kong SAR, China. *Quatern. Int.* **2004**, *117*, 41–54. [[CrossRef](#)]
- Yao, J. Climatic Indicators and Sedimentary Environment Studies Inferred from Transgressive and Regressive Sediments of Core LZ908, South Bohai Sea. Ph.D. Thesis, The University of Chinese Academy of Sciences (Institute of Oceanology, Chinese Academy of Sciences), Qingdao, China, 2014; pp. 1–118. (In Chinese with English abstract)
- Maher, B.A. Magnetic properties of some synthetic sub-micron magnetites. *Geophys. J. Int.* **1988**, *94*, 83–96. [[CrossRef](#)]
- Wang, J.; Liu, Z.C.; Jiang, W.Y.; Dong, L.X.; Zhu, M.Z.; Gao, F. A relationship between susceptibility and grain-size and minerals, and their paleo-environmental implications. *Acta Geogr. Sin.* **1996**, *51*, 155–163. (In Chinese with English abstract)
- Zhou, X.; Sun, L.G.; Huang, W.; Liu, Y.; Jia, N.; Cheng, W.H. Relationship between magnetic susceptibility and grain size of sediments in the China Seas and its implications. *Cont. Shelf Res.* **2014**, *72*, 131–137. [[CrossRef](#)]
- Wang, L.S.; Hu, S.Y.; Yu, G.; Ma, M.M.; Liao, M.N. Paleoenvironmental reconstruction of the radial sand ridge field in the South Yellow Sea (east China) since 45 ka using the sediment magnetic properties and granulometry. *J. Appl. Geophys.* **2015**, *122*, 1–10. [[CrossRef](#)]
- Wei, L.H.; Jiang, H.C.; He, H.L.; Xu, Y.R.; Gao, W.; Wei, Z.Y. Heinrich-5 Event revealed by high-resolution grain-size and magnetic susceptibility records and its significance of climate evolution in the last glacial at Hongtong, Shanxi, China. *Mar. Geol. Quat. Geol.* **2018**, *38*, 193–202. (In Chinese with English abstract)
- Hilton, J. A simple model for the interpretation of magnetic records in lacustrine and ocean sediments. *Quaternary Res.* **1987**, *27*, 160–166. [[CrossRef](#)]
- Liu, J.; Zhu, R.X.; Li, S.Q. Magnetic properties of the last glacial brown-yellow fine-grained sediment in the northern South Yellow Sea: Implication for its origin. *Mar. Geol. Quat. Geol.* **2002**, *22*, 15–20. (In Chinese with English abstract)

24. Liu, J.; Zhu, R.X.; Li, S.Q.; Chang, J.H. Magnetic mineral diagenesis in the post-glacial muddy sediments from the southeastern South Yellow Sea: Response to marine environmental changes. *Sci. China Ser. D* **2005**, *48*, 134–144. [[CrossRef](#)]
25. Liu, G.; Han, X.B.; Chen, Y.P.; Hu, B.Q.; Yi, L. Magnetic characteristics of core YSC-10 sediments in the central Yellow Sea mud area and implications for provenance changes. *Acta Sediment. Sin.* **2021**, *39*, 383–394. (In Chinese with English abstract)
26. Wang, Y. *Radiative Sandy Ridge Field on Continental Shelf of the Yellow Sea*; China Environmental Science Press: Beijing, China, 2002; pp. 1–373. (In Chinese)
27. Wang, Y. *Environment and Resource of the Radial Sand Ridge Field in the South Yellow Sea*; China Ocean Press: Beijing, China, 2014; pp. 1–293. (In Chinese)
28. Xia, F.; Yin, Y.; Wang, Q.; Zhang, Y.Z.; Liu, J.P. Sequence stratigraphy of the central part of North Jiangsu coasts since late MIS 3, eastern China. *Acta Geol. Sin.* **2012**, *86*, 1696–1712. (In Chinese with English abstract)
29. Xia, F.; Zhang, Y.Z.; Wang, Q.; Yin, Y.; Wegmann, K.W.; Liu, J.P. Evolution of sedimentary environments of the middle Jiangsu coast, South Yellow Sea since late MIS 3. *J. Geogr. Sci.* **2013**, *23*, 883–914. [[CrossRef](#)]
30. Zhang, G.; Yang, L.K.; Yan, Y.R.; Fan, Y.B.; Zhao, G. Variation characteristics of siltation movement at the Xiyang deep groove of Dafeng port in Yancheng, Jiangsu province. *J. Geol.* **2016**, *40*, 683–689. (In Chinese with English abstract)
31. The Office of 908 Special Project of the State Oceanic Administration of China. *Technical Regulations for Marine Bottom Sediment Investigation*; China Ocean Press: Beijing, China, 2006; pp. 1–63. (In Chinese)
32. Blott, S.J.; Pye, K. GRADISTAT: A grain size distribution and statistics package for the analysis of unconsolidated sediments. *Earth Surf. Proc. Land.* **2001**, *26*, 1237–1248. [[CrossRef](#)]
33. Xia, F. *Shallow Sequence Stratigraphy and Sedimentary Evolution of the Xiyang Tidal Channel in the Radial Sand Ridge Field*. Ph.D. Thesis, Nanjing University, Nanjing, China, 2016; pp. 1–187. (In Chinese with English abstract)
34. Xia, F.; Zhang, Y.Z.; Liu, D.Z. Rethinking on shallow sedimentary sequence and its evolution of the Xiyang tidal channel in the Radial Sand Ridge Field, South Yellow Sea. *Mar. Geol. Quat. Geol.* **2021**, *41*, 13–26. (In Chinese with English abstract)
35. Reineck, H.-E.; Singh, I.B. *Depositional Sedimentary Environments: With Reference to Terrigenous Clastics*, 2nd ed.; Springer: Berlin/Heidelberg, Germany, 1980; pp. 321–338.
36. Hori, K.; Saito, Y.; Zhao, Q.H.; Wang, P.X. Architecture and evolution of the tide-dominated Changjiang (Yangtze) River delta, China. *Sediment. Geol.* **2002**, *146*, 249–264. [[CrossRef](#)]
37. Berné, S.; Vagner, P.; Guichard, F.; Lericolais, G.; Liu, Z.X.; Trentesaux, A.; Yin, P.; Yi, H.I. Pleistocene forced regressions and tidal sand ridges in the East China Sea. *Mar. Geol.* **2002**, *188*, 293–315. [[CrossRef](#)]
38. Davis, R.A., Jr.; Dalrymple, R.W. *Principles of Tidal Sedimentology*; Springer: New York, NY, USA, 2012; pp. 79–149.
39. Meng, Q.Y.; Li, A.C.; Xu, F.J.; Zhou, X.J.; Li, C.S. Correlation between the grain size distribution and magnetic susceptibility of marine sediment core in the inner shelf of the East China Sea. *Sci. Tech. Rev.* **2009**, *27*, 32–36. (In Chinese with English abstract)
40. Yim, W.W.-S.; Ivanovich, M.; Yu, K.F. Young age bias of radiocarbon dates in pre-Holocene marine deposits of Hong Kong and implications for Pleistocene stratigraphy. *Geo-Mar. Lett.* **1990**, *10*, 165–172. [[CrossRef](#)]
41. Pigati, J.S.; Quade, J.; Wilson, J.; Timothy Jull, A.J.; Lifton, N.A. Development of low-background vacuum extraction and graphitization systems for ¹⁴C dating of old (40–60 ka) samples. *Quatern. Int.* **2007**, *166*, 4–14. [[CrossRef](#)]
42. Yi, L.; Jiang, X.Y.; Tian, L.Z.; Yu, H.J.; Xu, X.Y.; Shi, X.F.; Qin, H.F.; Deng, C.L. Geochronological study on Plio-Pleistocene evolution of Bohai Basin. *Quat. Sci.* **2016**, *36*, 1075–1087. (In Chinese with English abstract)
43. Long, H.; Zhang, J.R. Luminescence dating of Late Quaternary lake-levels in northern China. *Quat. Sci.* **2016**, *36*, 1191–1203. (In Chinese with English abstract)
44. Long, Z.R.; Wang, Z.B.; Tu, H.; Li, R.H.; Wen, Z.H.; Wang, Y.X.; Zhang, Y.; Lai, Z.P. OSL and radiocarbon dating of a core from the Bohai Sea in China and implication for Late Quaternary transgression pattern. *Quat. Geochronol.* **2022**, *70*, 101308. [[CrossRef](#)]
45. Gao, L.; Long, H. Luminescence chronology constraints on the sedimentary stratigraphy of the Yangtze River delta since MIS 5. *Quat. Sci.* **2023**, *43*, 33–45. (In Chinese with English abstract)
46. Wang, J.; Zhou, C.L.; Xu, X.B. *Research Report for the characteristics and sedimentary environments of the shallow strata of the 10,000-ton wharf at Zhongshan Port, Binhai County, Jiangsu Province*; Nanjing Normal University: Nanjing, China, 1995; pp. 1–20. (In Chinese)
47. Zhang, X. *Chronology and Sedimentary Environment Change in the Coastal-Shelf Areas of Eastern China Since 200 ka*. Ph.D. Thesis, China University of Geosciences, Wuhan, China, 2021; pp. 1–122. (In Chinese with English abstract)
48. He, L.; Ye, S.Y.; Xue, C.T.; Zhao, G.M.; Yang, S.X.; Amorosi, A. Sedimentology and evolution of the Holocene radial tidal sand ridge in the south Yellow Sea, China. *Front. Earth Sci.* **2023**, *10*, 1107495. [[CrossRef](#)]
49. Spratt, R.M.; Lisiecki, L.E. A Late Pleistocene sea level stack. *Clim. Past.* **2016**, *12*, 1079–1092. [[CrossRef](#)]
50. Liu, Q.S.; Deng, C.L. Magnetic susceptibility and its environmental significances. *Chin. J. Geophys.* **2009**, *52*, 1041–1048. (In Chinese with English abstract)
51. Murray-Wallace, C.V.; Woodroffe, C.D. *Quaternary Sea-Level Changes: A Global Perspective*; Cambridge University Press: New York, NY, USA, 2014; pp. 256–368.
52. Ke, X.K. Grain-size characteristics of tidal flat sediments. *Mar. Sci. Bull.* **1988**, *7*, 41–48. (In Chinese)
53. Chen, Y.Y.; Xia, F.; Zhang, Z.K.; Xu, Q.M.; Chen, S.Y. Research progress on distribution of Quaternary buried paleo-Yangtze River channels in the North Jiangsu-western South Yellow Sea. *Mar. Geol. Quat. Geol.* **2020**, *40*, 40–54. (In Chinese with English abstract)

54. Li, P.; Chen, G. Early diagenesis of Late Pleistocene dark-green stiff clay in the Yangzi River delta. *Oil Gas Geol.* **1995**, *16*, 313–318+401. (In Chinese with English abstract)
55. Xia, F.; Zhang, Y.Z.; Wang, L.; Liu, D.Z. Sedimentary sequence and age of core NTCJ1 in the Sheyang estuary, western South Yellow Sea: A re-interpretation. *Water* **2023**, *15*, 3617. [[CrossRef](#)]

Disclaimer/Publisher’s Note: The statements, opinions and data contained in all publications are solely those of the individual author(s) and contributor(s) and not of MDPI and/or the editor(s). MDPI and/or the editor(s) disclaim responsibility for any injury to people or property resulting from any ideas, methods, instructions or products referred to in the content.